

Synthesis, Characterization, Thermal, NLO and Quantum-Chemical Studies on *N*-Acetyl-2,6-bis(4-methoxyphenyl)-3-ethylpiperidin-4-one

V. MOHANRAJ^{1,2}, S. PONNUSWAMY^{1,*}, P. MUTHURAJA³ and M. DHANDAPANI³

¹P.G. and Research Department of Chemistry, Government Arts College (Autonomous), Coimbatore-641018, India

²Department of Chemistry, Manonmaniam Sundaranar University Constituent College, Kanyakumari-629 401, India

³P.G. and Research Department of Chemistry, Sri Ramakrishna Mission Vidyalaya College of Arts and Science (Autonomous), Coimbatore-641020, India

*Corresponding author: E-mail: kspons2001@gmail.com

Received: 18 April 2020;

Accepted: 19 May 2020;

Published online: 27 July 2020;

AJC-19980

Growth of a new organic single crystal of *N*-acetyl-2,6-bis(4-methoxyphenyl)piperidin-4-one (APM3EPO) is reported by using a slow evaporation method. The characterization of the crystal was done by IR and NMR spectra. Further, electronic spectrum and TG/DTA studies have also been carried out. The SHG efficiency of the crystal was found to be closer to that of standard KDP (potassium dihydrogen orthophosphate) using the modified Kurtz-Perry powder test employing Nd: YAG laser as the source of IR radiation. The calculated hyperpolarizability values were also projected to confirm the aptness of the crystal for non-linear optical applications. Optimization of the molecular structure of APM3EPO is done at the basic level of B3LYP/6-311(d,p) and the corresponding molecular properties such as HOMO-LOMO and Mulliken charge analyses are carried out at the same level of theory.

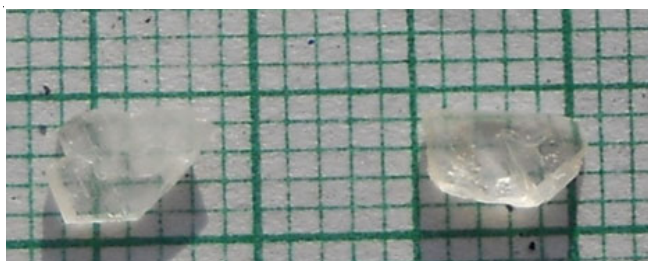
Keywords: Single crystal, Thermal analysis, Second harmonic generation, Density functional theory.

INTRODUCTION

In recent years, non-linear optical (NLO) materials are effectively used for the optical communication and related electro-optic applications [1-3]. The development of optical device technologies depends mainly on the growth of efficient NLO materials with high second harmonic generation (SHG) responses and discovery of novel and also more active materials [4]. Of late, the organic non-linear optical materials are of widespread interest because of their budding applications in electrical and electronic devices like optical moderator, optical switch and other photonic devices [5]. Use of organic molecules in the non-linear optical media is cost effective and possesses a number of advantages, like small dielectric constant and variety in organic structures. Perfect and suitable organic NLO materials can easily be obtained based on the chemical structures and properties which in turn due to their large structural diversity [6]. Quantum chemical methods suggest powerful implements for the computation of countless properties of molecules such as ground state geometry [7], reaction mecha-

nism, thermodynamics, *etc.* [8]. Molecular structures and their energies are determined, in general by the quantum chemists, using computer programs based on the mathematical methods [9,10]. These programs employ various methods to approximate wave functions, which are the solutions to wave equations of complex nature [11,12]. The wave function is intended by solving the wave equations innermost to quantum chemistry the non-relativistic Schrödinger equation [13].

Of late, we are working on the development of new organic NLO materials based on the skeleton of 2,6-diarylpiperidin-4-one [5,14]. In this paper, the crystal growth of *N*-acetyl-2,6-bis(4-methoxyphenyl)piperidin-4-one (APM3EPO) is reported (Fig. 1) using benzene as a solvent by slow evaporation method [14]. APM3EPO is characterized using the spectroscopic techniques *viz.* UV-vis, infrared (IR) and NMR (¹H NMR) spectroscopy. Furthermore, thermal (TG/DTA), NLO and quantum-chemical (DFT) studies are also carried out. The APM3EPO is a non-centrosymmetric material belonging to orthorhombic crystal system with space group *Pna2₁* [15].

Fig. 1. *N*-Acetyl 2,6-diaryl-3-ethyl piperidin-4-one (APM3EPO)

EXPERIMENTAL

The parent piperidin-4-one viz., 2,6-bis(4-methoxyphenyl)-piperidin-4-one, was prepared by following the well-known procedure [15]. 2,6-bis(4-methoxyphenyl)piperidin-4-one (3.39 g) was dissolved in dry benzene (70 mL) and also added triethylamine (2.78 g). To this solution, acetyl chloride (1.42 mL) was added immediately. The above reaction contents were refluxed on a water bath for about 12 h and the completion of the reaction was monitored by TLC (Scheme-I). The precipitated ammonium salt was removed by filtration. Further purification was carried out by washing the filtrate with more water (3-4 times). The organic layer was separated and dried using anhydrous sodium sulphate. The resulting solution was passed through a short column packed with silica and concentrated. Final purification of the obtained solid was done by recrystallization using the mixer of benzene and petroleum ether (60-80 °C) in the 9:1 ratio [15].

Crystal growth: Slow evaporation technique was used to get bigger crystals. Pure crystal of APM3EPO was used to prepare the saturated solution in benzene at 45 °C. The ensuing solution was collected by filtering through Whatman 41 filter paper. The final solution was allowed to evaporate slowly, in a dust free place, by covering the beaker with perforated sheet. Bulk transparent crystals with good optical quality were obtained after a period of ten days. The harvested crystals of APM3EPO are shown in Fig. 1.

RESULTS AND DISCUSSION

Transmission range is an important criterion to know the suitability of crystals for optical applications. Hence, an electronic absorption spectrum of APM3EPO is recorded using Double Beam UV-Vis spectrometer 2202 of Systronics Make in the range of 200 to 800 nm (Fig. 2). Strong absorption bands are observed in the near UV-region of the spectrum and assigned for π - π^* and n - π^* transitions. Electronic spectrum shows the

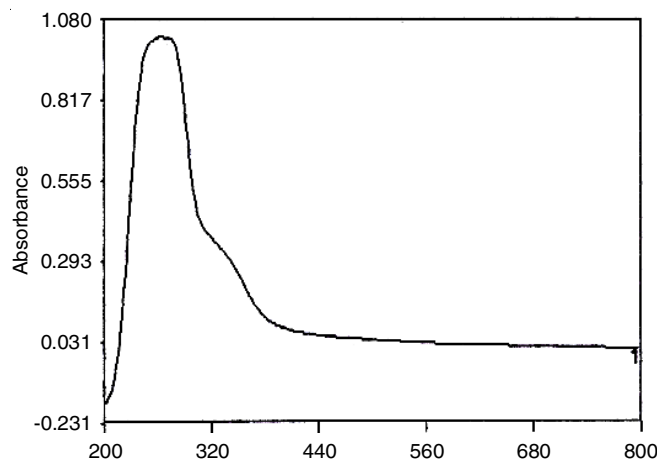


Fig. 2. UV-visible absorption spectrum of APM3EPO

absence of absorption band in the whole visible region up to 800 nm which in turn is an indication of very good transparency of the grown crystal. Thus, the material APM3EPO may be suitable for NLO applications.

FT-IR spectral analysis: Perkin-Elmer spectrometer was employed to record the FT-IR spectrum of the grown crystals by using KBr pellet technique in the range of 4000-400 cm^{-1} (Fig. 3). The peaks at 3027 and 2977 cm^{-1} were due to the asymmetric and symmetric stretching vibrations of aromatic C-H. Asymmetric and symmetric C-H stretching vibrations of -CH₃ and >CH₂ groups of APM3EPO are observed as a group of frequencies around 2801 cm^{-1} . Further, a strong band appearing at 1701 cm^{-1} has been assigned to the stretching vibration of carbonyl group.

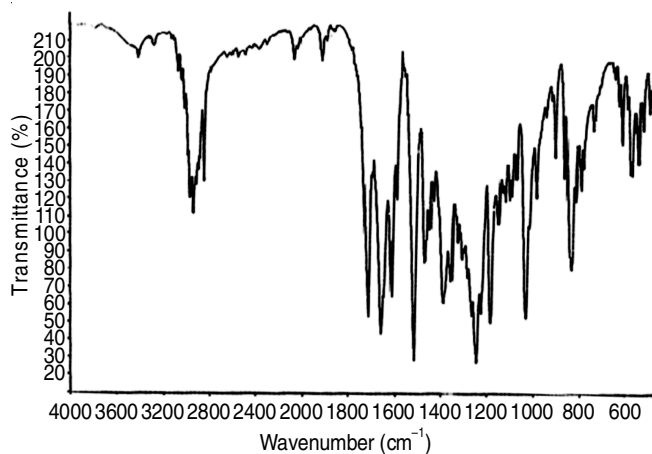
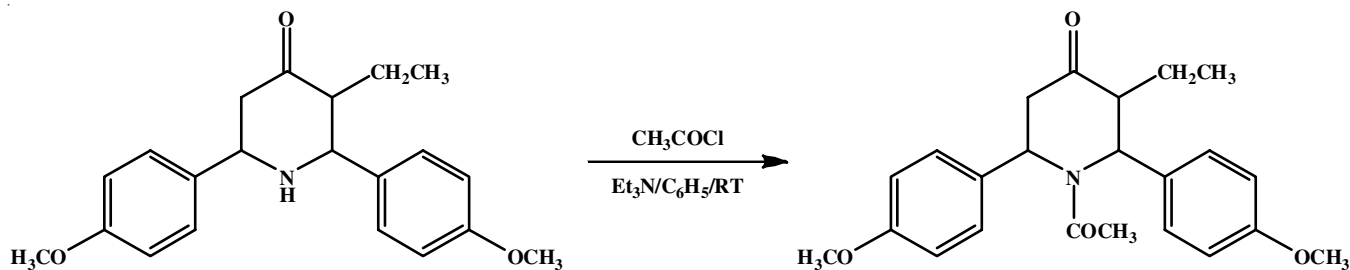


Fig. 3. FT-IR spectrum of APM3EPO

Scheme-I: Synthesis of *N*-acetyl-2,6-bis(4-methoxyphenyl)piperidin-4-one (APM3EPO)

^1H NMR analysis: The proton NMR spectrum of APM3EPO is reproduced in Fig. 4. The spectrum is recorded (δ ppm, solvent: CDCl_3) using Bruker-NMR spectrometer (500 MHz). The protons of CH_3 of C_3 -ethyl appear at 1.03 (t, 3H) and CH_2 of C_3 -ethyl appear at 1.70 (m, 1H) & 1.61 (m, 1H). The CH_3 of N -acetyl protons appear at 2.08 (s, 3H). Two doublets of a doublet (dd) appeared at 2.66 (1H) & 2.90 (1H) are due to the equatorial and axial protons, respectively at C_5 . A multiplet appearing at 2.98 (1H) has been assigned to the H_{3a} proton. The protons of two OCH_3 groups appear as singlet at 3.75 (3H) & 3.78 ppm (3H). The benzylic protons at C_2 (H_{2a}) & C_6 (H_{6a}) appear as broad signals at 5.00–6.00 ppm. The multiplet appearing between 6.71 and 7.16 ppm, accounting for eight protons has been assigned to aromatic protons.

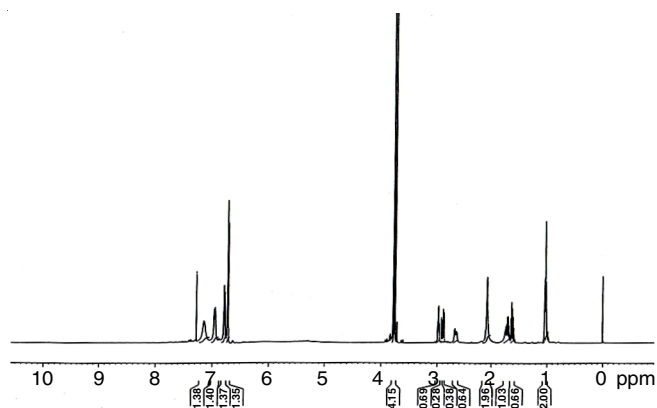


Fig. 4. ^1H NMR spectrum of APM3EPO

Thermal analysis: The compound APM3EPO was subjected to a TG/DTA analysis between 0°C and 500°C in a N_2 atmosphere (Fig. 5). This compound is likely to be unaffected up to the temperature of 220°C . Between 250°C and 450°C the compound gradually decomposed. A typical mass change of 57.45% occurred steadily due to the rupture of anisole moiety. Further, a steep change in mass of about 32.16% may be due to decomposition of piperidone moiety. The final residual mass change is 9.98% at 498°C due to possible decomposition of ammonium formate. A sharp endothermic peak was observed at 137.9°C in the DTA trace which might be due to the melting of the compound. Two more broad endothermic peaks are also

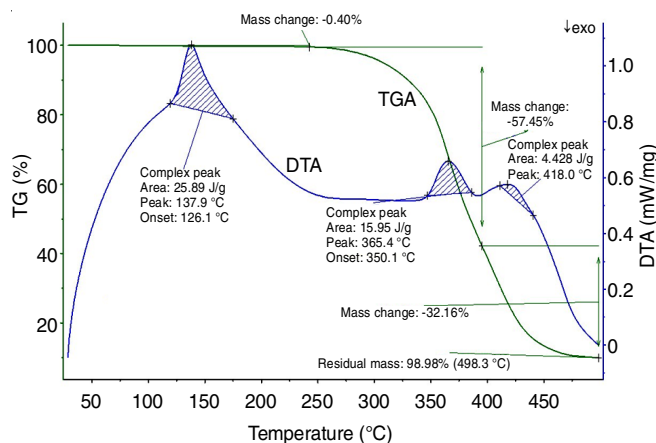


Fig. 5. TG/DTA analysis of APM3EPO

observed at 365.2°C and 418.0°C . Thus, the organic crystal is stable up to 220°C and may be appropriate for NLO applications.

SHG measurements: Second harmonic generation (SHG) efficiency of the powdered crystals of APM3EPO was measured by employing Kurtz and Perry technique [16]. The packed powdered crystal was illuminated using a Q-switched Nd:YAG laser as light source. In this measurement, a laser beam (wavelength = 1064; pulse width = 8 ns; pulse rate = 10 Hz) was allowed to fall on the sample cell and the laser energy fall on was 2.5 mJ/pulse. In this experiment, powdered KDP (potassium dihydrogen orthophosphate) was used as a reference material. For the given equal input beam energy, APM3EPO showed the SHG signal of 30.0 mV and the corresponding signal of KDP is 17 mV. Thus, SHG virtual efficiency of APM3EPO is established to be 1.77 times greater than that of KDP.

Quantum chemical studies: Quantum chemical calculation of APM3EPO was carried out with Gaussian 09, Revision E.01 program package with B3LYP/6-311 G(d,p) basic set [17].

Molecular geometry: The optimized molecular geometry and calculation of vibrational frequency were carried out for APM3EPO using Gaussian 09, Revision E.01 program [17]. Fig. 6 shows the DFT optimized structure of APM3EPO. The symmetry of ring is distorted by the electron donating $-\text{OCH}_3$ group on the phenyl ring and thereby alters the angles of piperidine ring at the point of attachment to 105.5° which is obviously smaller than tetrahedral angle. APM3EPO prefers distorted boat conformation in the solid state as evidenced from its crystal structure [15]. The atom O_1 of acetyl group attached to the nitrogen of piperidine ring forms a strong intramolecular hydrogen bonding with the neighbouring $\text{C}_{14}-\text{C}_{15}$ [$\text{C}_{14}-\text{H}_{15} \dots \text{O}_1$ (2.158 Å)] and this leads to the development of S (6) graph set [18]. The piperidone ring distortion is supported by the reduced dihedral angles of 45.5° and 32.6° for C_6-N_5-

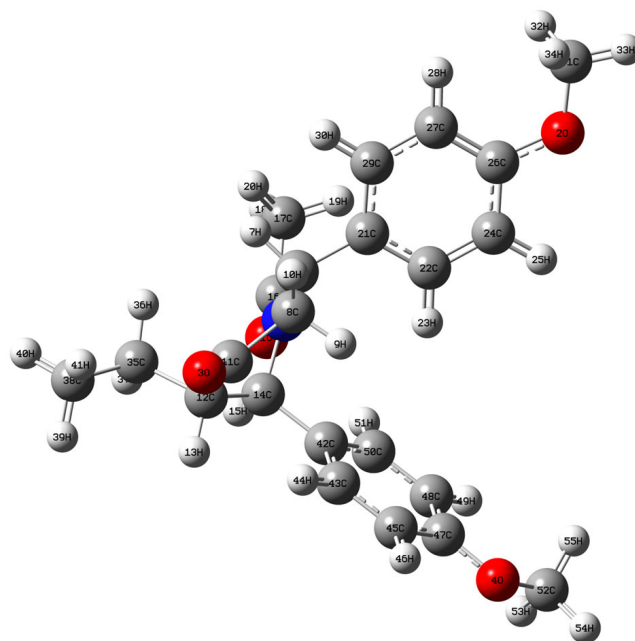


Fig. 6. Optimized structure of APM3EPO

C₁₄-C₁₂ & N₁-C₁₄-C₁₅-C₂₈, respectively. Bond angles of both methoxy substituted phenyl rings are found to be normal as reported in literature [15]. Based on the aggregate of bond angles, C₁₅-N₅-C₁₆, C₁₄-N₅-C₆ & C₆-N₅-C₁₆, which is found to be 359°, the hybridization of nitrogen of piperidone moiety is confirmed to be *sp*². This observation confirms the nitrogen lone pair delocalization with carbonyl group. Thus, the optimized parameters of APM3EPO are found to be almost equal to those determined experimentally [15], which also validate the theoretical studies.

HOMO and LUMO orbitals: The energy gap between HOMO and LUMO of APM3EPO (Fig. 7) was computed by using B3LYP/6-311 G(d,p) levels. High chemical reactivity of APM3EPO is indicated from its smaller energy gap and HOMO is localized on the molecule. In particular more electron density arises at one of the phenyl rings of APM3EPO while the localization of LUMO is mainly over the piperidone ring of APM3EPO. The energies of HOMO and LUMO are calculated as - 6.040 and - 0.895 eV, respectively. Negative HOMO and LUMO values revealed the molecule stability [13,18]. The energy gap of the molecule is 5.145 eV, which indicates the intermolecular charge transfer of the compound.

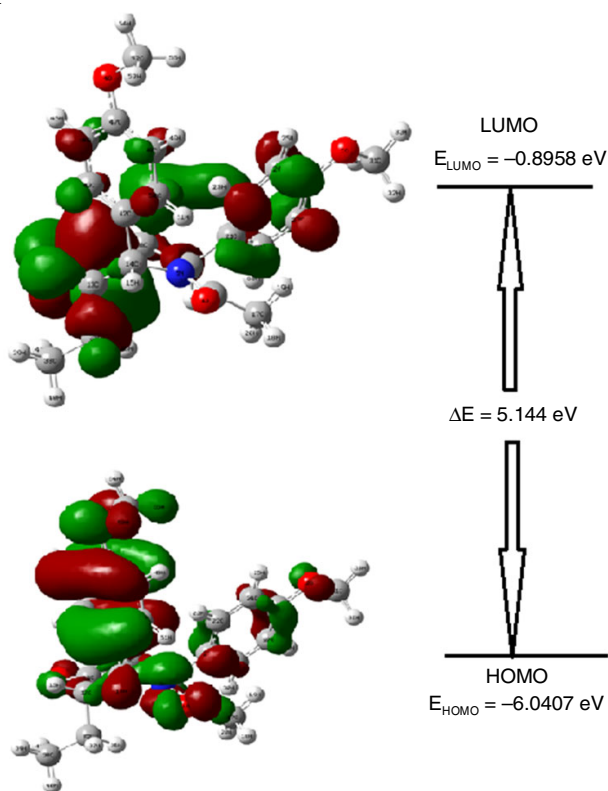


Fig. 7. HOMO-LUMO structure of APM3EPO

Mulliken atomic charges: Mulliken charge distribution of APM3EPO is given in Fig. 8. The carbon C₁₆, attached to the piperidone nitrogen, possesses the highest positive charge (+ 0.346 e) while another carbon holding electronegative oxygen O₃ as substituent also possesses positive charge of + 0.253 e. The methoxy substituted carbons C₂₆ and C₄₇ possess positive charge where as a negative charge is associated with carbons

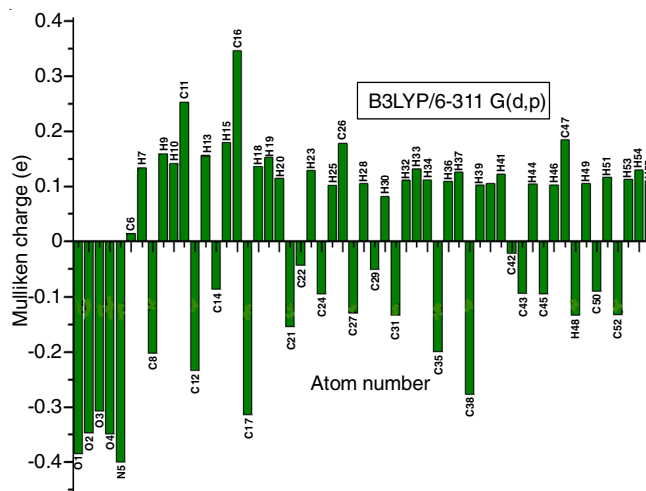


Fig. 8. Mulliken populations of APM3EPO

of methoxy groups (C₃₁ & C₅₂) due to the attached hydrogen atoms. All hydrogen atoms exhibit positive charge in which H₁₅ has the highest charge. This may be explained by the presence of intermolecular hydrogen bonding interaction in APM3EPO [18]. The nitrogen N₅ exhibits a highest negative charge of -0.400 e which causes the distortion of piperidone ring due to more electron density over the atom. Further, the electronegative oxygen atoms exhibit negative charge.

Hyperpolarizability: The dipole moment of APM3EPO was found to be 4.1677. The first hyperpolarizability of the material was also calculated at B3LYP/6-311 G(d,p) level of theory and found to be 2.118×10^{-30} esu. The β_{xxx} part has much influence on the molecular hyperpolarizability (Table-1). The value of hyperpolarizability is 13 times more when compared to that of urea when both were calculated at the same level of theory. This greater hyperpolarizability may be due to the intermolecular hydrogen bonding interaction found in the material [18].

TABLE-1
HYPERPOLARIZABILITY OF COMPONENTS AND
FIRST HYPERPOLARIZABILITY OF APM3EPO

Components	Values (esu)
β_{xxx}	1.6059×10^{-30}
β_{yyy}	8.43449×10^{-31}
β_{zzz}	-1.0485×10^{-31}
β_{xyy}	-1.1125×10^{-31}
β_{xxy}	-4.1364×10^{-32}
β_{xxz}	-1.5262×10^{-31}
β_{xzz}	3.3927×10^{-31}
β_{yzz}	4.5380×10^{-31}
β_{tot}	2.11862×10^{-30}

Conclusion

Slow evaporation method is followed to grow the single crystal of *N*-acetyl-2,6-bis(4-methoxyphenyl)piperidin-4-one (APM3EPO) material with fine optical quality using benzene as solvent at an ambient temperature. The material has been characterized using electronic, IR & ¹H NMR spectra. Further, TG/DTA and NLO studies have been carried out. Relative SHG

efficiency of APM3EPO was estimated to be 1.77 times higher than that of KDP. Density functional theory (DFT) methods with Gaussian 09, Revision E.01 program package B3LYP/6-311 G(d,p) basic set is used to carry out the theoretical studies. Interestingly, hyperpolarizability value is calculated to be 13 times greater than that of urea. Mulliken population analysis indicates that all hydrogen atoms exhibit positive charge in which H₁₅ possesses the highest and there by the presence of intermolecular hydrogen bonding interaction is proved.

CONFLICT OF INTEREST

The authors declare that there is no conflict of interests regarding the publication of this article.

REFERENCES

- J. Coleman, ed.: B.M. Deb, Calculation of the First- and Second-order Density Matrices, In: The Force Concept in Chemistry, Van Nostrand Reinhold: New York (1981).
- K. Udaya Lakshmi, N.P. Rajesh, K. Ramamurthi and B. Varghese, *J. Cryst. Growth*, **311**, 2484 (2009); <https://doi.org/10.1016/j.jcrysgro.2009.01.142>
- T.U. Devi, N. Lawrence, R. Ramesh Babu and K. Ramamurthi, *J. Cryst. Growth*, **310**, 116 (2008); <https://doi.org/10.1016/j.jcrysgro.2007.10.011>
- R. Uthrakumar, C. Vesta, R. Robert, G. Mangalam and S. Jerome Das, *Physica B*, **405**, 4274 (2010); <https://doi.org/10.1016/j.physb.2010.07.024>
- S. Ponnuswamy, V. Mohanraj, P. Sakthivel and A. Chandramohan, *Optik*, **125**, 5550 (2014); <https://doi.org/10.1016/j.ijleo.2014.07.064>
- R.G. Parr and W. Yang, Density-Functional Theory of Atoms and Molecules, Oxford University Press: Oxford (1989).
- A. Szabo and N.S. Ostlund, Modern Quantum Chemistry, Macmillan: New York (1982).
- T. Suthan, N.P. Rajesh, C.K. Mahadevan and G. Bhagavannarayana, *Spectrochim. Acta A Mol. Biomol. Spectrosc.*, **78**, 771 (2011); <https://doi.org/10.1016/j.saa.2010.12.012>
- R. Erdahl and V.H. Smith Jr., Density Matrices and Density Functionals, Reidel: Dordrecht (1987).
- P. Hohenberg and W. Kohn, *Phys. Rev.*, **136**, B864 (1964); <https://doi.org/10.1103/PhysRev.136.B864>
- M. Levy, *Proc. Natl. Acad. Sci. USA*, **76**, 6062 (1979); <https://doi.org/10.1073/pnas.76.12.6062>
- M. Foley and P.A. Madden, *Phys. Rev. B Condens. Matter*, **53**, 10589 (1996); <https://doi.org/10.1103/PhysRevB.53.10589>
- P. Muthuraja, M. Sethuram, M. Sethu Raman, M. Dhandapani and G. Amirthaganesan, *J. Mol. Struct.*, **1053**, 5 (2013); <https://doi.org/10.1016/j.molstruc.2013.09.004>
- S. Ponnuswamy, V. Mohanraj, S.S. Ilango, M. Thenmozhi and M.N. Ponnuswamy, *J. Mol. Struct.*, **1081**, 449 (2015); <https://doi.org/10.1016/j.molstruc.2014.10.063>
- K. Ravichandran, S. Ponnuswamy, R. Rajesh, V. Mohanraj and M.N. Ponnuswamy, *Acta Crystallogr.*, **E66**, o275 (2010).
- S.K. Kurtz and T.T. Perry, *J. Appl. Phys.*, **39**, 3798 (1968); <https://doi.org/10.1063/1.1656857>
- M.J. Frisch, G.W. Trucks, H.B. Schlegel, G.E. Scuseria, M.A. Robb, J.R. Cheeseman, G. Scalmani, V. Barone, B. Mennucci, G.A. Petersson, H. Nakatsuji, M. Caricato, X. Li, H.P. Hratchian, A.F. Izmaylov, J. Bloino, G. Zheng, J.L. Sonnenberg, M. Hada, M. Ehara, K. Toyota, R. Fukuda, J. Hasegawa, M. Ishida, T. Nakajima, Y. Honda, O. Kitao, H. Nakai, T. Vreven, J.A. Montgomery, Jr., J.E. Peralta, F. Ogliaro, M. Bearpark, J.J. Heyd, E. Brothers, K. N. Kudin, V. N. Staroverov, T. Keith, R. Kobayashi, J. Normand, K. Raghavachari, A. Rendell, J.C. Burant, S.S. Iyengar, J. Tomasi, M. Cossi, N. Rega, J.M. Millam, M. Klene, J.E. Knox, J.B. Cross, V. Bakken, C. Adamo, J. Jaramillo, R. Gomperts, R.E. Stratmann, O. Yazyev, A.J. Austin, R. Cammi, C. Pomelli, J.W. Ochterski, R.L. Martin, K. Morokuma, V. G. Zakrzewski, G. A. Voth, P. Salvador, J.J. Dannenberg, S. Dapprich, A.D. Daniels, O. Farkas, J.B. Foresman, J.V. Ortiz, J. Cioslowski and D.J. Fox, Gaussian 09, Revision E.01, Gaussian, Inc.: Wallingford CT (2013).
- P. Muthuraja, T.J. Beaula, T. Shanmugavadivu, V.B. Jothy and M. Dhandapani, *J. Mol. Struct.*, **1137**, 649 (2017); <https://doi.org/10.1016/j.molstruc.2017.02.067>